Kinetic, equilibrium, and thermodynamic studies of untreated watermelon peels for removal of copper(II) from aqueous solution

Nurul Izza Taib[a,*], Nur Arifah Rosli[b], Nurul Izzati Saharrudin[b], Nyliawani Mohd Rozi[c], Nur Amalin Ainin Kasdiehram[d], Nadhirah Nur Tasnim Abu Nazri[a]

[a]*Faculty of Applied Sciences, Universiti Teknologi MARA, Perak Branch, Tapah Campus, 35400 Tapah Road, Perak, Malaysia, Tel. +60-183920120; email: izza257@uitm.edu.my*
[b]*Faculty of Applied Sciences, Universiti Teknologi MARA, 40450 Shah Alam, Selangor, Malaysia*
[c]*Faculty of Science and Technology, Universiti Kebangsaan Malaysia, 43600 Bangi, Selangor, Malaysia*
[d]*Faculty of Mechanical Engineering, Universiti Teknologi MARA, 40450 Shah Alam, Selangor, Malaysia*

Received 8 September 2020; Accepted 2 April 2021

ABSTRACT

In this study, the watermelon peels (WP) were used as an adsorbent without any chemical or physical treatment for Cu^{2+} removal from the aqueous solution. Removal of Cu^{2+} has been evaluated with respect to initial metal concentration, contact time, pH, and temperature using batch-adsorption techniques. The maximum adsorption process was favorable at pH 5. As for the effects of concentration on WP, the maximum adsorption for Cu^{2+} has shown at 70 mg/L. Sorption equilibrium reach rapidly with 79.5% Cu^{2+} removal in 75 min. The adsorption isotherms could be fitted well by the Langmuir model with a maximum adsorption capacity of 357.14 mg/g. The R_L value in the present investigation was less than one, which indicates that the adsorption of the Cu^{2+} onto WP is favorable. Sorption energies analyses were conducted using Dubinin–Radushkevich (D–R) and Temkin isotherm models. It was found that the sorption energies of Cu^{2+} on WP obeyed D–R isotherm with $R^2 = 0.998$, mean adsorption energy, b = 0.0018 mol^2/J^2, and mean free energy, $E = 0.0167$ kJ/mol which vividly proved that the adsorption process was physisorption in nature. The kinetics models fitted with pseudo-second-order suggesting that the adsorption might involve chemical sorption. The positive value of Gibbs free energy shows the reaction is non-spontaneous and the positive value of enthalpy shows the adsorption process to be exothermic in nature. Fourier transform infrared analysis showed that carboxyl and hydroxyl functional groups were involved in the adsorption of Cu^{2+}. The present study showed that WP is an easy synthesis, economic, and an effective adsorbent for Cu^{2+} removal from aqueous solutions.

Keywords: Adsorption; Kinetics; Thermodynamics; Isotherm; Watermelon peels

1. Introduction

Heavy metals are the most common pollutants caused by various industrial activities, have raised severe environmental impacts [1,2]. It has been intensively investigated from the point of view of their persistence and toxicity. Owing to their high solubility in water and non-biodegradable, they can easily deposit and spread in the environment for a longer time.

As a consequence, they enter the food chain threatening public health resulting in several diseases and also lead to severe ecological hazards [3,4]. Copper is one of the essential elements to human life and living organisms in trace amounts, but at over 1.3 mg/L [5], it is potential to cause stomach and intestine problems, neurotoxicity, jaundice, mucosal irritation, lung cancer, and liver toxicity [6,7]. Copper is released from a wide range of industries such as mining, smelting, electroplating, and brass manufacture that can give negative effects on the water [8]. According to the Safe Drinking Water

---

* Corresponding author.

Act, the permissible limit of copper in drinking water is set to be 1.3 mg/L [9]. Moreover, the contamination of copper can affect the marine ecosystem and causes damage to the kidneys, liver, gills, and the nervous system of fishes [10]. Therefore, it is crucial to treat wastewater before its discharge into water streams.

There are many conventional technologies such as chemical coagulation, photodegradation, precipitation, flocculation, activated sludge process, adsorption, membrane separation, and ion exchange processes that have been tested for removal of heavy metals [11,12]. Each of these methods has some limitations and is inadequate to deal with the wastewater treatment problem [13]. Adsorption is known to be an effective method for the removal of heavy metal due to its stability, utility, economics, ease of operation, and performances [11,14,15].

Sorption of copper with different materials has been reported in the literature. The use of natural organic matter-modified Al_2O_3 nanoparticles was studied by Khan et al. [16] and maximum uptake of 62.50 mg/g was obtained. Gupta and Gogate [10] who also studied the adsorption of copper by calcium hydroxide-activated watermelon and citric acid-activated watermelon achieved an uptake of 31.25 and 27.027 mg/g at pH 5.0, respectively. Another reports are also found in the literature using the lemon peel for copper removal, with a maximum uptake capacity of 13.2 mg/g at pH 4.0 [17].

Considering it is an abandoned, readily available, low cost, environment-friendly bio-material, fruit peels such as banana peel [18], lemon peel [17], orange peel [19], jack fruit peel [20], and mango peel [21] has been reported as potential and low-cost adsorbents for removal of heavy metals. Watermelon (*Citrullus lanatus*) being the heaviest and largest fruit is one of the cheapest and most abundantly available in Malaysia with an average production of 154,416 tons [22]. Being the flesh is edible, sweet and it appears in red color, it is often used in juices, and salad preparation. However, watermelon peel (WP) is commonly known as a waste product that possesses no commercial value thus becoming a source of pollution. WP is composed of pectin (carboxyl), citrulline, cellulose (hydroxyl), proteins, and carotenoid [23–25] that capable attract heavy metal ions. Therefore, its conversion to adsorbent in wastewater treatment offers both economic feasibility and waste handling advantages.

In this study, naturally abundant watermelon peel (WP) was used without any pre-treatment prior to the tests as an attempt to reduce the cost of the adsorption process. The main objective of the study was to investigate the feasibility of using WP as an adsorbent in the removal of Cu^{2+} ions; to evaluate various experimental parameters that affect the adsorption process, including the contact time, initial concentration, pH, and temperature; to assess the efficacy of various kinetic models (pseudo-first-order and pseudo-second-order); to determine the applicability of isotherm models (Langmuir, Freundlich, Dubinin–Radushkevich (D–R), and Temkin); and to specify the thermodynamic feasibility of the adsorption process in accordance with thermodynamic parameters (Gibbs energy ($\Delta G°$), enthalpy ($\Delta H°$), and entropy ($\Delta S°$)). Characterization of WP was carried out by using Fourier transform infrared (FTIR), X-ray diffraction (XRD), and thermogravimetric analysis (TGA) to characterize the watermelon peels.

2. Materials and methods

2.1. Preparation of adsorbent using watermelon peel

The adsorbent used was untreated watermelon peel (WP) which was obtained from a local market in Tapah, Perak, Malaysia. The watermelon peel (WP) was then cut into small pieces and washed thoroughly with distilled water to remove dirt and suspended materials. Then, the peels were dried in the oven for 24 h at 100°C. The dried peels were then cooled, blended into a fine powder, and used as such for adsorption studies.

2.2. Preparation of stock solution

A stock solution of Cu^{2+} (500 mg/L) was prepared by dissolving a predetermined amount of $CuSO_4·5H_2O$ in 2 L of distilled water. The required solutions for the adsorption experiment were prepared by diluting a stock solution to the certain required concentrations. Fresh dilutions were used for each adsorption experiment.

2.3. Characterization

The presence of active functional groups was done by using attenuated total reflection spectrophotometer (Perkin Elmer spectrum one spectrometer, Waltham, MA, USA) in the range of 4,000–800 cm^{-1}. Powder X-ray powder diffraction (PXRD) was used to analyze the structure and identify the phase purity of WP. The samples were placed on a flat plate while intensity data were collected as a function of the Bragg angle, θ, in the range 2θ = 10°–70° with a step size of 0.013° using a PAN analytical *X'*pert PRO diffractometer (Netherlands) in Bragg–Brentono geometry using Cu Kα radiation wavelength $\lambda\alpha1 = 1.5405$ Å, $\lambda\alpha2 = 1.5443$ Å. Thermal stability of the samples was measured using SETARAM SET-SYS (LCT 10257-2) under nitrogen flow (35 mL/min) with a heating rate 20°C/min from 40°C to 900°C.

2.4. Batch adsorption studies

Adsorption experiments were conducted by contacting 200 mg of dried WP with 50 mL of Cu^{2+} solutions of known concentration (20–250 mg/L) in 150 mL Erlenmeyer flask, shaken on an orbital shaker at 100 rpm for 4 h at 298 K. Kinetic studies were conducted in continuously stirred flask containing 50 mL of Cu^{2+} solutions at 298 K by using orbital shaker at 100 rpm at variable contact time (15–90 min) at a concentration of Cu^{2+} (100 mg/L). The effect of temperature was obtained in a continuously stirred flask containing 50 mL Cu^{2+} at a concentration of 50 mg/L from 308 to 328 K with constant WP dosage (0.20 g). In the study of the pH effect, only the pH of Cu^{2+} solutions was adjusted with 0.1 M HCl and 0.1 M NaOH. The mixture was shaken for 1 h on a stirrer plate. The supernatant of the reaction mixture was separated by centrifugation for 2 min at 1,200 rpm. After filtering the mixture, the concentration of Cu^{2+} in the filtrate was determined by flame atomic

absorption spectrometry (atomic absorption spectrometer analyst 400; Perkin Elmer). The removal percentage (%) and adsorption capacity of WP (q_e, mg/g) were determined by using Eqs. (1) and (2), respectively:

$$\text{Removal}(\%) = \frac{(C_0 - C_e)}{C_0} \times 100 \tag{1}$$

$$q_e = \frac{(C_0 - C_e)}{m} V \tag{2}$$

where q_e is the mg of Cu^{2+} biosorbed per g of WP (mg/g), C_0 (mg/L) is the initial Cu^{2+} concentrations, C_e (mg/L) is the final Cu^{2+} concentrations, V (L) is the volume of the solution, and m is the mass of the WP (g) in the reaction mixture.

3. Results and discussion

3.1. Fourier transform infrared

Figs. 1a and b show the FTIR spectrum before and after adsorption of Cu^{2+} on the surface of WP, respectively. The intense and broad peak at 3,373 cm^{-1} (Fig. 1a) attributed to the presence of –OH stretching vibrations of cellulose, pectin, and lignin of WP. The peak located at 2,920 cm^{-1} represents the stretching vibrations of –C–H of the methyl group. The presence of band at 1,733 cm^{-1} are characteristic of C=O of carboxylic acid or ester group which may be from pectin. The band at 1,620 and 1,430 cm^{-1} characteristics of asymmetric and symmetric vibrations of –COO from carboxylic groups. Meanwhile, bands between 1,300 and 1,000 cm^{-1} are assigned to the C–O and C–O–C stretching vibrations in carboxylic acids, alcohols, phenols, or ester groups.

Fig. 1b shows that after adsorption of Cu^{2+}, there is a shift in the intensity of –OH and carbonyl bands confirming their role in adsorption. It showed that –OH, –COOH are the groups showing changes before and after the adsorption and hence these are the most active groups in WP.
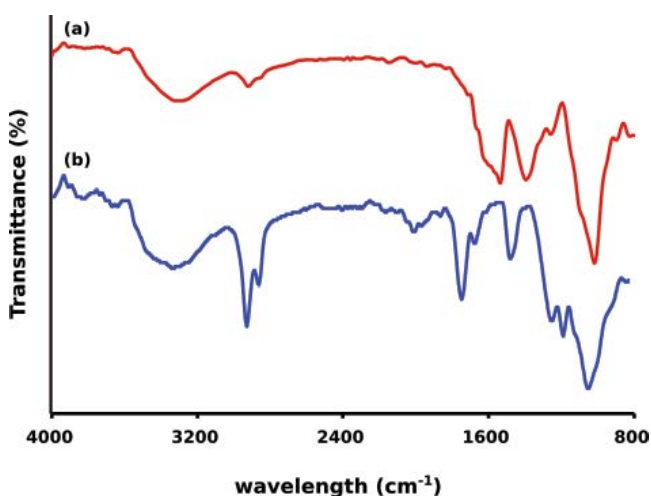
3.2. Powder X-ray diffraction

There is a visible difference in the XRD diffraction pattern of WP before and after adsorption with respect to the shifting of peaks, decrease in intensity of the peaks, and disappearance of peaks. The XRD of the untreated WP is shown in Fig. 2a. The sharpness and the intensity of peaks indicate the semi-crystalline nature of the untreated WP with diffraction peaks appearing at 2θ = 22.2°, 38.4°, 44.6°, 65.0°, and 78.2°. The XRD spectra of Cu^{2+} loaded WP is presented in Fig. 2b. The diffractogram showed a typical amorphous in nature. The XRD data of the Cu^{2+} loaded WP have evidence of the crystalline nature of WP changing into amorphous nature after adsorption and this suggests the adsorption of Cu^{2+} on the surface of WP. This finding suggests the loss of crystallinity due to the adsorption of Cu^{2+} on WP.

3.3. Thermogravimetric analysis

The TGA of the WP as a function of temperature is shown in Fig. 3. It can be seen that WP are stable at high temperatures. The loss of mass of WP before and after Cu^{2+} adsorption is very similar, the behavior is the same for both samples, however, the WP before Cu^{2+} adsorption presents a slightly higher loss of mass. The loss of mass between 27°C and 150°C could be attributed to the removal of physisorbed water initially present in the WP; before Cu^{2+} adsorption, the weight loss is 0.36 wt.% and after Cu^{2+} adsorption is 1.4 wt.%. Between 151°C and 600°C, a

Fig. 1. FTIR spectra of (a) before and (b) after adsorption of Cu^{2+} onto the surface of WP.
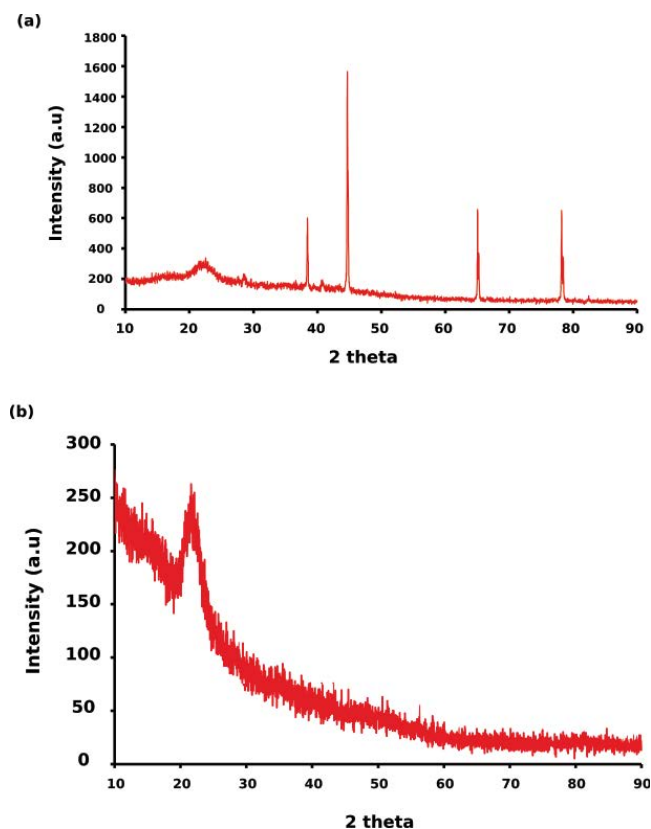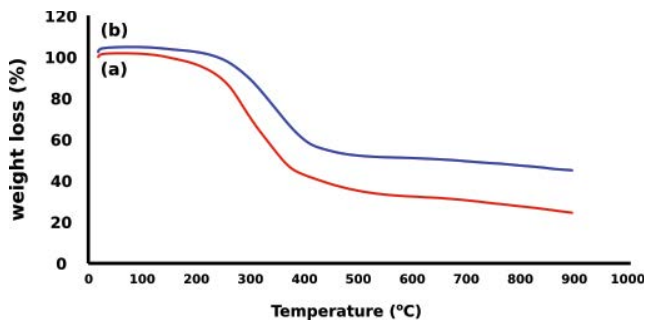
Fig. 2. XRD spectra of (a) before and (b) after adsorption of Cu^{2+} onto the surface of WP.

Fig. 3. TGA curve of (a) before and (b) after adsorption of Cu^{2+} onto the surface of WP.

Fig. 4. Point of zero charges (pH_{pzc}) of the WP.

significant weight loss is observed for both, it is 67.1 wt.% before Cu^{2+} adsorption and 52.7 wt.% after Cu^{2+} adsorption. The loss could be due to the organic matter decomposition as well as volatile substance releases proceeding from inorganic compound decomposition. During this stage, the complete degradation of the cellulose occurs (at about 300°C). Lignin pyrolysis occurs at about 400°C, while hemicellulose decomposes at a considerably lower temperature. Finally, between 601°C and 900°C, the loss step is 7.82 wt.% before Cu^{2+} adsorption and 5.93 wt.% after Cu^{2+} adsorption, the loss could be caused be attributed to slow decomposition of the remaining heavy components, which may consist of stable micronutrients like metal oxide. The total weight loss is 75% for WP before Cu^{2+} adsorption and 60% for WP before Cu^{2+} adsorption.

3.4. Point of zero charge

The pH at the point zero charges (pH_{pzc}) is a characteristic to determine the interfacial properties which help to deduce which ionic species can be adsorbed by the WP at desired pH. A mass of 0.10 g of WP was added into 50 mL of 0.1 N sodium chloride (NaCl) as electrolyte buffered to pH 2.00–12.00 by adding HCl (0.01 M) and NaOH (0.01 M). The pH_{pzc} of the WP was determined by plotting pH (final pH – initial pH) vs. pH initial. The suspension was then kept stirred 24 h at room temperature and the final pH of each suspension was measured.

As can be seen from Fig. 4, the pH_{pzc} of untreated WP was 6.40 which reflected the surface of WP was acidic. The adsorption of Cu^{2+} can be attributed to the presence of OH, and COO^- groups on the surface of WP. This is in agreement with the FTIR results (Fig. 1) that carboxylic acids are present in abundance within WP. At pH below 6.40, the surface of WP is positively charged due to protonation and at pH above 6.40, it is negatively charged. Hence, it is predicted that the adsorption of cationic species by WP will be favored at pH above 6.40. On the other hand, the adsorption of anionic species by WP will be appropriate at pH below 6.40 because of the electrostatic interactions.

3.5. Effect of pH

Fig. 5 illustrates the effect of pH on the adsorption of Cu^{2+} onto WP. The obtained results show that the adsorption of Cu^{2+} onto WMR increased gradually with an increase
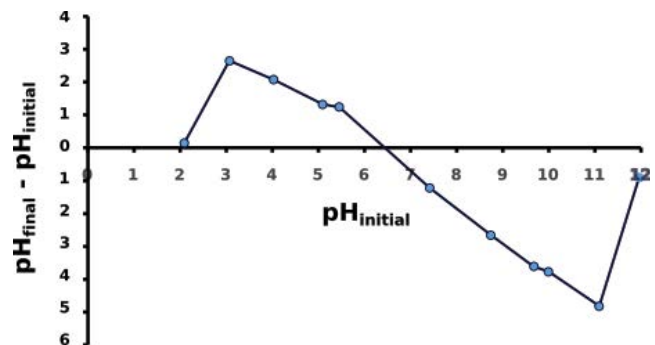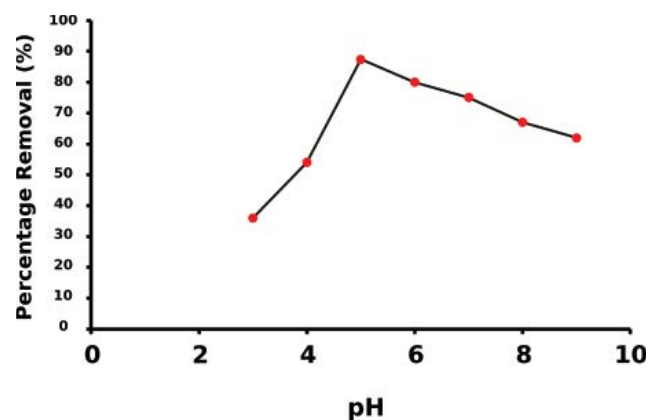

Fig. 5. Effect of pH on the percentage removal of Cu^{2+}. Conditions: 50 mL Cu^{2+} of 100 mg/L, agitation time: 3 h, agitation speed: 100 rpm, sorbent dosage: 0.2 g, temperature: 298 K, and pH: 3.0–9.0.

in solution pH up to pH 5.0 after which further increase in pH values exhibited minor decreases up to pH 9. The percentage removal increases from 36% at pH 3.0 to 87% at pH 5.0, then it decreases to 62% by increasing the pH up to 9. Lower percentage removal at low pH may be either due to excess concentration of H^+ ions competing with the Cu^{2+} for adsorption sites. Moreover, at solution pH < pH_{pzc} = 6.40, the surface of WP was positively charged, and thus, the repulsion between the Cu^{2+} and the positive surface of WP may have occurred and decreased the Cu^{2+} percentage removal. At higher pH till the optimum, the surface of WP was likely to have negative surface charges and became increasingly favorable for Cu^{2+} adsorption due to electrostatic forces of attraction between the negatively charged surface of the WP and Cu^{2+}. At pH 6.0, the adsorbent gives lower removal percentage which may be due to the hydrolysis of Cu^{2+} forming the colloidal complex which is very difficult to be adsorbed on the WP.

However, in this study the optimum removal was observed at pH 5.0 which is lower than pH_{pzc} of WP, therefore, the adsorption of Cu^{2+} onto WP could be governed via non-electrostatic interaction such as chemisorption and precipitation [26].

3.6. Effect of contact time

The effect of contact time on percentage removal is presented in Fig. 6, which indicates that maximum Cu^{2+} uptake is attained at 75 min. Adsorption increases from 69.29% for 30 min of exposure up to 79.51% for 75 min. In the initial stages of contact time, the removal of Cu^{2+} is rapid and gradually decreases with time until saturation occurs. It can be seen that within 75 min, the major sorption process was completed and the curve became flattened. The increase in Cu^{2+} uptake can be attributed to the large number of vacant adsorption sites initially available on the WP surface, which become progressively occupied until saturation is attained in accordance with the work of Meena et al. [27]. By extending the contact time beyond the optimum state, the process of removal of heavy metals was not significantly effective. As the adsorption process went on, the available site of WP decreases, the rate of diffusion of Cu^{2+} onto WP decreases, so does the rate of adsorption. On the other hand, the adsorption percentage was decreased due to the accumulation of metal ion species [28].

3.7. Effect of initial concentration

Fig. 7 shows the percentage removal (%) of Cu^{2+} from aqueous solution at a different initial concentration from 20 to 250 mg/L for 4 h. It is evident from Fig. 7 that the Cu^{2+} percentage removal generally decreases with increasing Cu^{2+} concentration. The percentage removal (%) was at a peak when the Cu^{2+} concentration was 70 mg/L with 83.0% and start to decrease to 45.6% at 250 mg/L. At lower concentrations, a higher extent of adsorption was observed due to the higher driving force in terms of the availability of a sufficient binding site. Meanwhile, at higher concentrations, there is a competition for adsorption, and hence, more Cu^{2+} ions are left unadsorbed in the solution due to the adsorption site became limited which causes the saturation of the adsorption site.

3.8. Adsorption kinetics studies

For adsorption kinetics studies, it is related to the contact time as it plays an important role affecting the efficiency
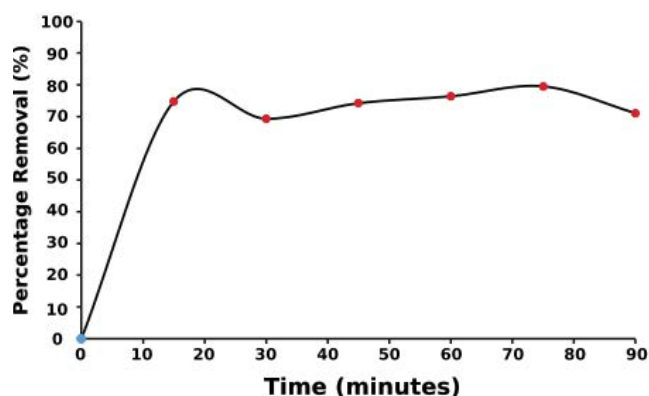
of adsorption. The kinetic of Cu^{2+} adsorption on WP were modeled with pseudo-first-order and pseudo-second-order models.

For the pseudo-first-order rate equation of Langergen is shown as [29]:

$$\log\left(q_e - q_t\right) = \log q_e - \frac{k_1}{2.303}t \tag{3}$$

Pseudo-second-order equation can be expressed as [29]:

$$\frac{t}{q_t} = \frac{1}{k_2 q_e^2} + \frac{t}{q_e} \tag{4}$$

where q_e is the amount of Cu^{2+} adsorbed at equilibrium (mg/g), q_t is the amount of Cu^{2+} adsorbed at time t and k_1 is the pseudo-first-order reaction rate constant and k_2 pseudo-second-order reaction rate constant. The k_1 and theoretical $q_{e,cal}$ values for Cu^{2+} adsorption by WP can be calculated from the intercept and slope of the $\log(q_e - q_t)$ vs. t plot. The k_2 and theoretical $q_{e,cal}$ values can be calculated from the intercept and slope of the t/q_t vs. t plot (Fig. 8).

The linear regression coefficient, R^2, and parameters of pseudo-first-order and pseudo-second-order kinetic models are listed in Table 1. A very poor correlation between
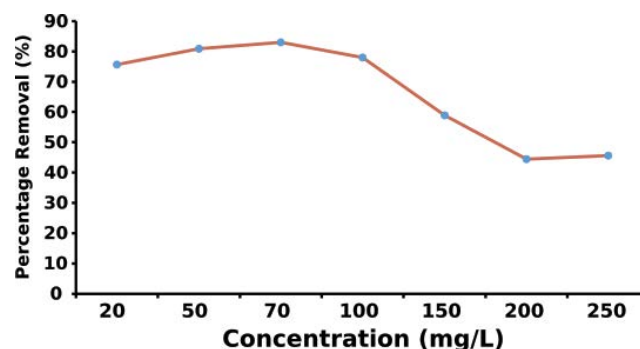

Fig. 7. Effect of initial concentration on the percentage removal of Cu^{2+}. Conditions: 50 mL Cu^{2+}, initial concentration: 20–250 mg/L, agitation time: 4 h, agitation speed: 100 rpm, sorbent dosage: 0.2 g, temperature: 298 K, and pH 6.0.

Fig. 6. Effect of contact time on the percentage removal of Cu^{2+}. Conditions: 50 mL Cu^{2+} of 100 mg/L, agitation time: 15–90 min, agitation speed: 100 rpm, sorbent dosage: 0.2 g, temperature: 298 K, and pH 6.0.
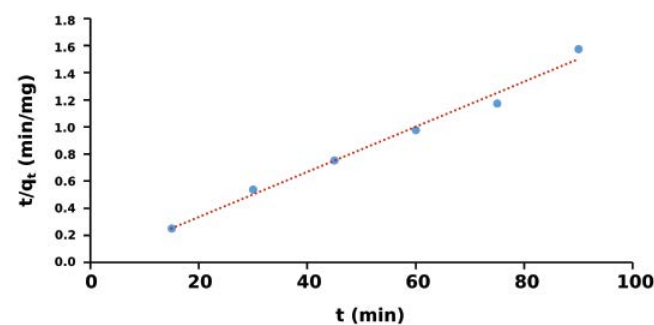

Fig. 8. Pseudo-second-order kinetics for the adsorption of Cu^{2+} onto WP. Conditions: 50 mL Cu^{2+}, agitation time: 15–90 min, initial concentration: 50 mg/L, agitation speed: 100 rpm, sorbent dosage: 0.2 g, temperature: 298 K, and pH 6.0.

Table 1
Adsorption kinetic parameters for the removal of Cu^{2+} by using WP

	Pseudo-first-order			Pseudo-second-order	
	k_1 (min^{-1})	$q_{e,cal}$ (mg/g)	R^2	k_2	$q_{e,cal}$
0.0088	−0.001612	4.3782	0.9878	0.1213	59.8802

experimentally q_e values (64.00 mg/g) and the pseudo-first-order kinetic (4.38 mg/g) was observed with negative reaction constant ($k_1 = -0.0016$), indicating the unsatisfactory of the pseudo-first-order model. Additionally, the strong agreement between q_e values obtained from pseudo-second-order model (59.88 mg/g) and the experimental values (64.00 mg/g) confirmed the suitability of pseudo-second-order model in fitting the kinetic data.

These results indicated that the adsorption of Cu^{2+} onto WP is more likely controlled by the chemisorption process [30,31] that involved sharing of electrons or by covalent forces through exchanging of electrons between adsorbent and adsorbate. This demonstrated that Cu^{2+} can be bound to different binding sites on the WP. Similar kinetic behaviors were also reported for adsorption of Cu^{2+} onto pomegranate peel [32], lemon peel [33], orange peel [34], and banana peel [18].

3.9. Adsorption isotherm studies

The adsorption models are powerful tools to give some insights into the adsorption process and to derive important parameters revealing the adsorption mechanism. To examine the interaction between Cu^{2+} and WP, adsorption equilibrium data were fitted to the Langmuir, Freundlich, D–R, and Temkin models. The parameters of Langmuir, Freundlich, D–R, and Temkin isotherm along with regression coefficient R^2 are given in Table 2.

3.9.1. Langmuir isotherm

The Langmuir model assumes that monolayer adsorption occurs on a homogeneous surface with a finite number of adsorption sites and negligible mutual interactions between the adsorbed molecules [32]. The linear form of the Langmuir equation is given as [35]:

$$\frac{C_e}{q_e} = \frac{1}{bq_{max}} + \frac{C_e}{q_{max}} \tag{5}$$

where q_e is the amount of Cu^{2+} adsorbed at equilibrium (mg/g), C_e is the concentration of Cu^{2+} at equilibrium (mg/L), q_{max} (mg/g) is the maximum Cu^{2+} uptake (mg/g) corresponding to complete coverage of the adsorptive sites and b (L/mg) is the Langmuir constant related to the energy of adsorption. Values b and q_{max} can be determined from the intercept and slope of the plot C_e/q_e vs. C_e (Fig. 9), respectively.

It was found that correlation coefficient values 0.9942, suggesting that the adsorption of Cu^{2+} onto WP follows Langmuir isotherm, which suggests that the adsorption takes place in the form of monolayer coverage on the surface of the

Table 2
Adsorption isotherm parameters values for the adsorption of Cu^{2+} onto WP

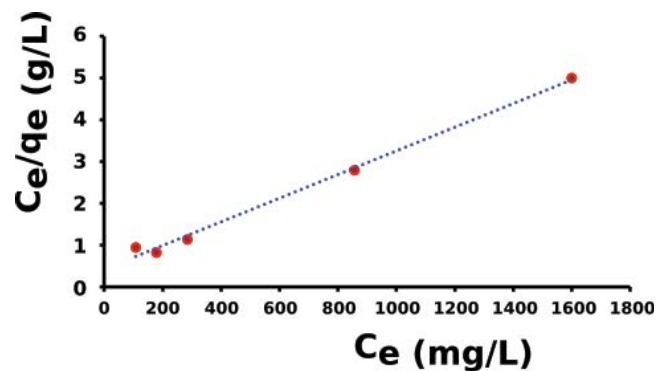| Isotherm model	Estimated isotherm parameters	
Langmuir	q_{max} (mg/g)	357.14
	b (L/mg)	6.66×10^{-3}
	R^2	0.9942
Freundlich	K_f (L/g)	8.8039
	n	1.989
	R^2	0.9431
Dubinin–Radushkevich	q_D (mg/g)	313.03
	β (mol^2/J^2)	0.0018
	E (kJ/mol)	0.0167
	R^2	0.9983
Temkin	A_T (L/mg)	0.0286
	B (J/mol)	90.659
	b_T	27.343
	R^2	0.9797

Fig. 9. Langmuir plot for the adsorption of Cu^{2+} onto WP.

WP. The results also demonstrate the homogeneous nature of the WP surface, in which each Cu^{2+} molecule/WP has equal adsorption activation energy [28,36]. The calculated monolayer capacity (q_{max}) of the WP for the Cu^{2+} is comparable to the maximum adsorption obtained from the experimentally (366.65 mg/g). Based on the Table 2, the following values are $q_{max} = 357.14$ mg/g, $b = 6.66 \times 10^{-3}$ L/mg, and $R^2 = 0.9942$.

The essential characteristics of the Langmuir isotherm can be interpreted via the dimensionless equilibrium parameter R_L, which is defined as:

$$R_L = \frac{1}{1 + bC_0} \tag{6}$$

The type of the adsorption isotherm is determined by the value range of: unfavourable ($R_L > 1$), linear ($R_L = 1$), favorable ($0 < R_L < 1$), and irreversible ($R_L = 0$). The obtained R_L values at different Cu^{2+} concentrations are equal to be 0.045–0.304 for all initial concentrations, indicating that the adsorption of Cu^{2+} onto WP is a favorable process. The R_L values gradually decrease as the concentrations were increased, showing

Table 3
Comparison of adsorption capacity of Cu^{2+} onto watermelon peel with other sorbents from the literature

Adsorbent	Adsorption capacity (mg/g)	References
Banana peel	28.57	[18]
Orange peel	3.19	[19]
Potato peel	0.3887	[38]
Pomegranate peel	30.12	[32]
Banana peel	8.24	[39]
Watermelon rind	5.73	[39]
Sweet lime peel	37.45	[40]
Lemon peel	13.25	[17]
Watermelon shell	9.54	[41]
Lemon peel	8.24	[41]
Watermelon peel	357.14	This study

that a higher initial concentration of Cu^{2+} may improve the adsorption process [37].

To estimate the adsorption ability of the WP, we compared the obtained data (Table 3) on the removal of Cu^{2+} onto WP with other non-conventional adsorbents reported in the literature. It is evident from the table that WP has got the highest adsorption capacity of Cu^{2+} onto WP among all the adsorbents.

3.9.2. Freundlich isotherm

The Freundlich model assumes that molecules are adsorbed on the heterogeneous surfaces of adsorbent based on different sites with different adsorption energies and there is an interaction between the adsorbed molecules. The linear form of Freundlich adsorption isotherm is given as [35,42]:

$$q_e = K_F C_e^{1/n_F} \tag{7}$$

which can be simplified as:

$$\ln q_e = \ln K_f + \frac{1}{n_F} \ln C_e \tag{8}$$

where q_e is the amount of Cu^{2+} adsorbed at equilibrium (mg/g) and C_e is the concentration of Cu^{2+} in the aqueous phase at equilibrium (mg/L). The n value indicates the favorability of adsorption; if $n > 1$ then adsorption is favorable and K_f (mg/g) is the adsorption capacity of the sorbent [32]. The K_F and n_F can be determined from the intercept and slope of the plot $\ln q_e$ vs. $\ln C_e$ given in Fig. 10. Table 2 shows the following values are $K_F = 8.8039$ L/g, $n_F = 1.989$, and $R^2 = 0.9431$. Thus, the Cu^{2+} adsorption process using WP can be considered as a favorable process [43] and indicates the physical adsorption of Cu^{2+} onto WP [44]. This may suggest a distribution of surface sites that causes a decrease in adsorbent–adsorbate interaction with increasing surface density [45]. It was found that the correlation coefficient was less than 0.99, indicating that the Freundlich model was not applicable to the present study.
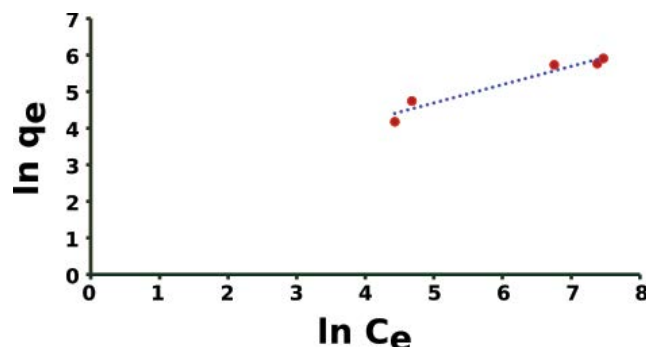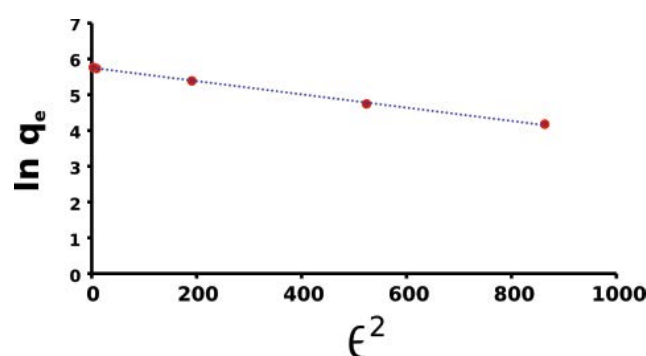

Fig. 10. Freundlich plot for the adsorption of Cu^{2+} onto WP.

Fig. 11. Dubinin–Radushkevich (D–R) plot for the adsorption of Cu^{2+} onto WP.

3.9.3. Dubinin–Radushkevich

The D–R approach was applied to distinguish the physical and chemical adsorption of metal ions based on its mean free energy E per molecule of the adsorbent. The equation is given as follows [46,47]:

$$\ln q_e = \ln q_D - \beta \left[RT \ln \left(1 + \frac{1}{C_e} \right) \right]^2 \tag{9}$$

$$\ln q_e = \ln q_D - \beta \in^2 \tag{10}$$

where q_e is the equilibrium Cu^{2+} concentration on the adsorbent (mg/g), q_D is the maximum adsorption capacity (mg/g), β is the D–R constant related to mean adsorption energy (mol^2/J^2), C_e is the equilibrium concentration of Cu^{2+} ions (mg/L), R is the universal gas constant (8.314 J/mol K), T is temperature at 298.15 K. The values of q_D and β were calculated from the intercept and slope of $\ln q_e$ vs. $\in^2$ plot, while that of $\in$ (Polanyi potential) was calculated using:

$$\in = RT \ln \left(1 + \frac{1}{C_e} \right) \tag{11}$$

The mean free energy of adsorption E (kJ/mol) was estimated using:

$$E = \frac{1}{\sqrt{2\beta}} \qquad (12)$$

From the D–R plot shown in Fig. 11, the following values were estimated: q_D = 313.03 mg/g, β = 0.0018 mol²/J² which is an indication of a physical adsorption process, and the R^2 = 0.998. The D–R model with higher correlation coefficient values, R^2 = 0.998 proves a better choice in explaining sorption energies.

The adsorption process is said to be dominated by physisorption for the energy values less than 8 kJ/mol, by a chemical ion-exchange mechanism for those between 8 and 16 kJ/mol, and by chemical particle diffusion for the greater than 16 kJ/mol [48]. The energy value obtained according to this model (0.0167 kJ/mol) was less than 8 kJ/mol. This isotherm assumes multilayer adsorption of Cu^{2+} onto WP, which generally involves weak van der Waals forces between adsorbates and adsorbents, indicative of the physical adsorption process. This result will be confirmed by the thermodynamic study.

3.9.4. Temkin isotherm

The Temkin adsorption isotherm assumes that the heat of adsorption of all molecules in the layer would decrease linearly with the sorption coverage due to indirect interaction between absorbent–absorbate [18]. The equation can be described as follows:

$$q_e = \frac{RT}{b_T}\ln\left(A_T C_e\right) \qquad (13)$$

The linear form of the isotherm can be represented as follows:

$$q_e = B\ln A_T + B\ln C_e \qquad (14)$$

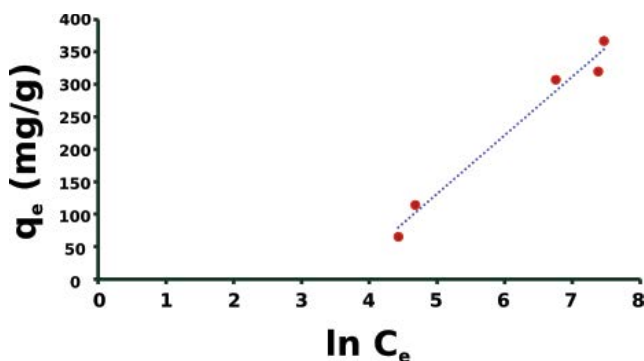where $B = RT/b_T$, A_T is the Temkin equilibrium binding constant corresponding to the maximum bonding energy (L/mg), B is the Temkin constant related to the heat of sorption (J/mol), b_T is the Temkin isotherm constant, R is the universal gas constant (8.314 J/mol K), T is the temperature at 298.15 K. Therefore, by plotting q_e vs. $\ln C_e$, enables the determination of the A_T and B.

From the Temkin plot (Fig. 12), the following values were estimated: A_T = 0.0286 L/mg, B = 90.659 J/mol, and b_T = 27.343 which is an indication of a physical adsorption and the R^2 = 0.980. The value of A_T is 0.0286 L/mg indicating a weak bonding of the adsorbate onto the medium. The value of B constant was found to be less than 8 kJ/mol proved a weak interaction between Cu^{2+} and WP. The adsorption energy is positive for Cu^{2+} adsorption from the aqueous solution, which indicates that the adsorption is exothermic. Meanwhile, b_T value is <8 kJ indicating that the physical adsorption process is involved [49]. However, it contradicts with the fitting of the equation of pseudo-second-order model which indicates adsorption is chemisorption type. Since the Temkin isotherm assumes that the heat of adsorption changes linearly with adsorbate concentration, it can be inferred from the results plotted in Fig. 12 that the heat of adsorption increased linearly for WP.

3.10. Thermodynamic studies

The effect of temperature on the removal of Cu^{2+} was investigated between 298 and 328 K by keeping the experimental conditions constant. As seen in Fig. 13, the percentage removal decreased with temperature rise. The thermodynamic parameters of adsorption of Cu^{2+} onto WP were derived from the experimental data obtained at 298, 308, 318, and 328 K to deduce the nature and thermodynamic feasibility of the adsorption process. The standard free energy change ($\Delta G°$), enthalpy change ($\Delta H°$), and entropy change ($\Delta S°$) were estimated using Eqs. (15) and (16) [50,51]:

$$k_d = \frac{q_e}{C_e} \qquad (15)$$

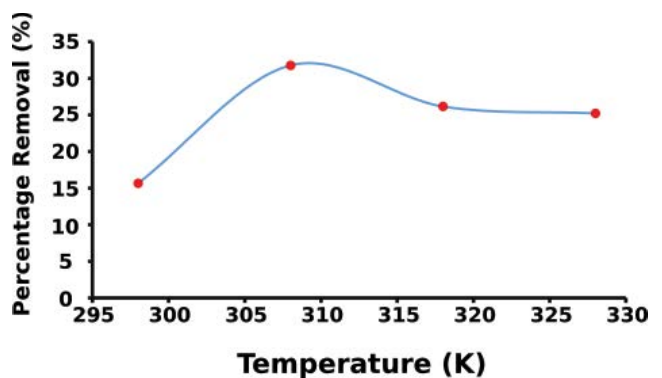Fig. 12. Temkin plot for Cu^{2+} removal from aqueous solutions by WP.

Fig. 13. Effect of temperature on the percentage removal of Cu^{2+}. Conditions: 50 mL Cu^{2+}, agitation time: 3 h, initial concentration: 50 mg/L, agitation speed: 100 rpm, sorbent dosage: 0.2 g, temperature: 298–328 K, and pH 6.0.

$$\ln k_d = -\frac{\Delta G°}{RT} = \frac{\Delta S°}{R} - \frac{\Delta H°}{T} \qquad (16)$$

where k_d is the distribution coefficient, q_e is the concentration of Cu^{2+} adsorbed onto WP at equilibrium (mg/L), C_e is the equilibrium of Cu^{2+} in the liquid phase (mg/L), R is the universal gas constant (8.314 J/mol K), and T is the absolute temperature (K). By using Van't Hoff plot ($\ln k_d$ vs. $1/T$), the values of $\Delta H°$ and $\Delta S°$ were calculated from the slope and intercept and presented in Table 4.

It is observed that the removal of Cu^{2+} increases from 15.7% to 31.8% with the increase in temperature from 298 to 308 K. However, the Cu^{2+} removal decreases with the increase in temperature beyond 308 K. The values of k_d decreased with the increasing of temperature suggests that the Cu^{2+} adsorption capacity of WP decreased with the rise of temperature and this suggested that the adsorption process was exothermic in nature. The observation can be attributed to the weakening of bonds between the Cu^{2+} molecules and active sites of WP at high temperatures that may lead to the decreased surface active sites as well as adsorption capacity [52]. The negative value of $\Delta H°$ (–13.665 kJ/mol) confirmed the exothermic nature of the adsorption process confirming that physical forces occur during the adsorption of Cu^{2+} onto WP [32,33] and consistent with the reduction amount of Cu^{2+} adsorbed at elevated temperature. This is in good agreement with n value derived from Freundlich isotherm and is further confirmed by the mean free energy, E from the D–R model.

The positive $\Delta G°$ values suggest that the adsorption process was a non-spontaneous adsorption reaction. The increase in $\Delta G°$ values with increasing temperature suggests

that adsorption of Cu^{2+} onto WP is more favorable at higher temperature [53] which suggests that the temperature influenced the adsorption of Cu^{2+} onto WP.

The negative $\Delta S°$ (–0.063 kJ/mol K) value revealed the decrease in the randomness at solid–solution interface through the adsorption of Cu^{2+} onto WP. This indicates that adsorption leads to an increase in the Cu^{2+} order at the solid–liquid interface during the adsorption process on WP and is supportive of the interaction between Cu^{2+} and WP. As the temperature increases, the mobility of metal ions increases causing the ions to escape from the solid phase to the liquid phase. Therefore the amount of metals that can be adsorbed will decrease [54]. The exothermic process during the adsorption of copper onto various adsorbents has also been reported by other researchers [33]. Also, low value of $\Delta S°$ suggests no remarkable change on entropy.

3.11. Mechanism of the adsorption

Many factors may influence the sorption behavior of Cu^{2+} onto WP, such as adsorbent surface properties, steric effect, hydrogen bonding, and van der Waals forces. Macromolecular components of the WP include mainly cellulose (20%), hemicelluloses (23%). Lignin (10%), pectin (13%), and silica free minerals (12%) which contain various functional groups such as hydroxyl (cellulose) and carboxyl (pectin) [55]. The presence of –COOH and OH groups on the surface of WP surface are expected to play important role in the removal of Cu^{2+} from an aqueous solution. It is suggested that the Cu^{2+} adsorption mechanism can be assigned to the interaction of electrostatic attractions between the positively charged (Cu^{2+}) and negatively charged (–COO$^-$ and –OH$^-$) on the surface of the WP as suggested in Fig. 14. The mechanism of sorption is accomplished by deprotonation of hydroxyl or carboxyl groups followed by metal chelation.

4. Conclusion

This study reveals that untreated WP can be non-hazardous agro-material and an inexpensive adsorbent for the removal of Cu^{2+} ions from aqueous solutions. The presence of –COOH and –OH was confirmed by FTIR. The removal of Cu^{2+} achieved equilibriums within 75 min with a percentage removal 79.5% with a mass of 200 mg of WP. The equilibrium data were perfect fit better with the Langmuir isotherm model with the monolayer adsorption capacity (q_e) of WP
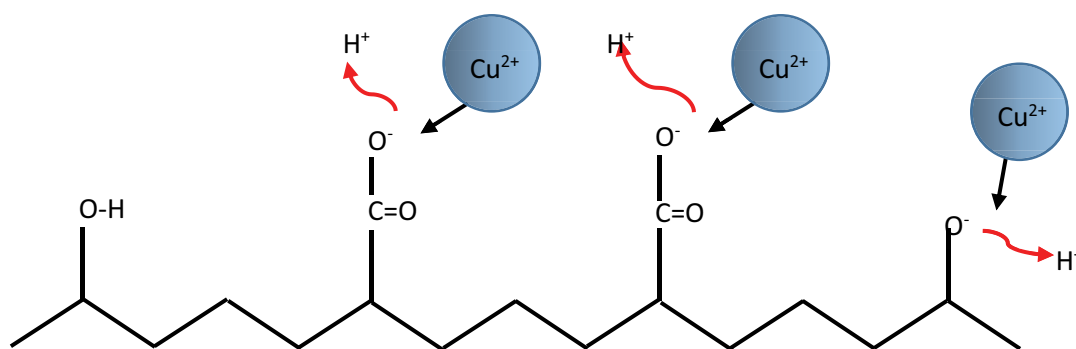
Table 4
Thermodynamic parameters values for the adsorption Cu^{2+} onto WP

Temperature (K)	$\Delta G°$ (kJ/mol)	$\Delta H°$ (kJ/mol)	$\Delta S°$ (J/mol K)
298	4.969	–13.66489	–0.062530425
308	5.594		
318	6.220		
328	6.84509		

Fig. 14. Possible mechanism of the Cu^{2+} on the WP surface.

was found to be 357.14 mg/g. Thus, this adsorption is done in a monolayer on homogenous surfaces. Kinetic data fitted well with pseudo-second-order kinetics, which indicated that chemisorption might have a dominant role for Cu^{2+} removal from an aqueous solution. $\Delta G°$ values for Cu^{2+} ions were identified as positive; thus it was identified that adsorption was non-spontaneous. Negative values for $\Delta H°$ indicate that the system release energy to surroundings (exothermic) and negative $\Delta S°$ indicates a more regular state of Cu^{2+} ions over the WP surface. Meanwhile, the sorption energies data of Cu^{2+} adsorption on WP can be modelled by D–R, and Temkin isotherms. The data in the linearized forms of D–R gave satisfactory correlation coefficients for the studied concentrations. Sorption energy value (B), mean free energy (E), and heat of sorption (β) were estimated as 0.0018 mol^2/J^2, 0.0167 kJ/mol, and 90.659 J/mol, respectively which reveals the physisorption process dominates chemisorption and ion exchange. Hence, these observations suggest that WP adsorbent which has a low-cost value is more effective for the removal of Cu^{2+} ions from aqueous solutions.

Acknowledgments

References

[1] R.M. Salim, A.J.K. Chowdhury, R. Rayathulhan, K. Yunus, M.Z.I. Sarkar, Biosorption of Pb and Cu from aqueous solution using banana peel powder, Desal. Water Treat., 57 (2016) 303–314, doi: 10.1080/19443994.2015.1091613.

[2] M. Naushad, A. Mittal, M. Rathore, V. Gupta, Ion-exchange kinetic studies for Cd(II), Co(II), Cu(II), and Pb(II) metal ions over a composite cation exchanger, Desal. Water Treat., 54 (2015) 2883–2890.

[3] M.D. Machado, S. Janssens, H.M.V.M. Soares, E.V. Soares, Removal of heavy metals using a brewer's yeast strain of *Saccharomyces cerevisiae*: advantages of using dead biomass, J. Appl. Microbiol., 106 (2009) 1792–1804.

[4] P.I. Girginova, A.L. Daniel-da-Silva, C.B.Lopes, P. Figueira, M. Otero, V.S. Amaral, E. Pereira, T. Trindade, Silica coated magnetite particles for magnetic removal of Hg^{2+} from water, J. Colloid Interface Sci., 345 (2010) 234–240.

[5] M.M. Beppu, E.J. Arruda, R. Vieira, N.N. Santos, Adsorption of Cu(II) on porous chitosan membranes functionalized with histidine, J. Membr. Sci., 240 (2004) 227–235.

[6] X. Zeng, E. Ruckenstein, Supported chitosan-dye affinity membranes and their protein adsorption, J. Membr. Sci., 117 (1996) 271–278.

[7] M.L.P. Dalida, A.F.V. Mariano, C.M. Futalan, C.-C. Kan, W.-C. Tsai, M.-W. Wan, Adsorptive removal of Cu(II) from aqueous solutions using non-crosslinked and crosslinked chitosan-coated bentonite beads, Desalination, 275 (2011) 154–159.

[8] P.K. Ingle, C. Gadipelly, A.V.K. Rathod, Sorption of copper(II) from aqueous solution onto *Arachis hypogaea* husk, Desal. Water Treat., 55 (2015) 401–409.

[9] P.D. Johnson, M.A. Watson, J.M. Brown, I.A. Jefcoat, Peanut hull pellets as a single use sorbent for the capture of Cu(II) from wastewater, Waste Manage., 22 (2002) 471–480.

[10] H. Gupta, P.R. Gogate, Intensified removal of copper from waste water using activated watermelon based biosorbent in the presence of ultrasound, Ultrason. Sonochem., 30 (2016) 113–122.

[11] F. Fu, Q. Wang, Removal of heavy metal ions from wastewaters: a review, J. Environ. Manage., 92 (2011) 407–418.

[12] S. Babel, T.A. Kurniawan, Low-cost adsorbents for heavy metals uptake from contaminated water: a review, J. Hazard. Mater., 97 (2003) 219–243.

[13] P.R. Rout, P. Bhunia, R.R. Dash, A mechanistic approach to evaluate the effectiveness of red soil as a natural adsorbent for phosphate removal from wastewater, Desal. Water Treat., 54 (2015) 358–373.

[14] G. Akkaya, F. Guzel, Bioremoval and recovery of Cu(II) and Pb(II) from aqueous solution by a novel biosorbent watermelon (*Citrullus lanatus*) seed hulls: kinetic study, equilibrium isotherm, SEM and FTIR analysis, Desal. Water Treat., 51 (2013) 7311–7322.

[15] R. Lakshmipathy, N.C. Sarada, Metal ion free watermelon (*Citrullus lanatus*) rind as adsorbent for the removal of lead and copper ions from aqueous solution, Desal. Water Treat., 57 (2015) 15362–15372.

[16] S. Khan, Z. Dan, Y. Mengling, Y. Yang, H. Haiyan, J. Hao, Isotherms, kinetics and thermodynamic studies of adsorption of Ni and Cu by modification of Al_2O_3 nanoparticles with natural organic matter, Fullerenes Nanotubes Carbon Nanostruct., 26 (2018) 158–167.

[17] S. Meseldzija, J. Petrovic, A. Onjia, T. Volkov-Husovic, A. Nesic, N. Vukelic, Utilization of agro-industrial waste for removal of copper ions from aqueous solutions and mining-wastewater, J. Ind. Eng. Chem., 75 (2019) 246–252.

[18] M.A. Hossain, H.H. Ngo, W. Guo, T.V. Nguyen, Removal of copper from water by adsorption onto banana peel as bioadsorbent, Int. J. Geomate, 2 (2012) 227–234.

[19] A. Habib, N. Islam, A. Islam, A.M.S. Alam, Removal of copper from aqueous solution using orange peel, sawdust and bagasse, Pak. J. Anal. Environ. Chem., 8 (2007) 21–25.

[20] B.S. Inbaraj, N. Sulochana, Carbonised jackfruit peel as an adsorbent for the removal of Cd(II) from aqueous solution, Bioresour. Technol., 94 (2004) 49–52.

[21] M. Iqbal, A. Saeed, S.I. Zafar, FTIR spectrophotometry, kinetics and adsorption isotherms modeling, ion exchange, and EDX analysis for understanding the mechanism of Cd^{2+} and Pb^{2+} removal by mango peel waste, J. Hazard. Mater., 164 (2009) 161–171.

[22] M. Bahari, M.Y. Rafii, G.B. Saleh, M.A. Latif, Combining ability analysis in complete diallel cross of watermelon (*Citrullus lanatus* (Thunb.) Matsum. & Nakai), Sci. World J., 2012 (2012) 1–6, doi: 10.1100/2012/543158.

[23] S. Rangil, J.C. Kumar, K.S. Nandpuri, A study on the influence of tne structural chemical constituents of the skin of water melon (*Citrullus lanatus* Sch.) fruit on the incidence of its blossom-end-rot and cracking, Indian J. Horticult., 32 (1975) 98–101.

[24] R. Lakshmipathy, A.V. Vinod, N.C. Sarada, Watermelon rind as biosorbent for removal of Cd^{2+} from aqueous solution: FTIR, EDX, and kinetic studies, J. Indian Chem. Soc., 90 (2013) 1147–1154.

[25] A.M. Rimando, P.M. Perkins-Veazie, Determination of citrulline in watermelon rind, J. Chromatogr. A, 1078 (2005) 196–200.

[26] T. Phuengprasop, J. Sittiwong, F. Unob, Removal of heavy metal ions by iron oxide coated sewage sludge, J. Hazard. Mater., 186 (2011) 502–507.

[27] A.K. Meena, G.K. Mishra, P.K. Rai, C. Rajagopal, P.N. Nagar, Removal of heavy metal ions from aqueous solution using carbon aerogel as an adsorbent, J. Hazard. Mater., 122 (2005) 161–170.

[28] B.H. Hameed, A.T.M. Din, A.L. Ahmad, Adsorption of methylene blue onto bamboo–based activated carbon: kinetics and equilibrium studies, J. Hazard. Mater., 141 (2007) 819–825.

[29] N.I. Taib, N. Kantasamy, S.M. Sumari, N.M. Rafi, Adsorption of Arsenic(V) and Phosphate onto $MgAlNO_3$-LDHs, 2012 IEEE Symposium on Humanities, Science and Engineering Research, Kuala Lumpur, 2012, pp. 333–338.

[30] R.M. Ali, H.A. Hamad, M.M. Hussein, G.F. Malash, Potential of using green adsorbent of heavy metal removal from aqueous solutions: adsorption kinetics, isotherm, thermodynamic, mechanism and economic analysis, Ecol. Eng., 91 (2016) 317–332.

[31] L. Sha, G. Xueyi, F. Ningchuan, T. Qinghua, Adsorption of Cu²⁺ and Cd²⁺ from aqueous solution by mercapto-acetic acid modified orange peel, Colloids Surf., B, 73 (2009) 10–14.

[32] S. Ben-Ali, I. Jaouali, S. Souissi-Najar, A. Ouederni, Characterization and adsorption capacity of raw pomegranate peel biosorbent for copper removal, J. Cleaner Prod., 142 (2017) 3809–3821.

[33] A. Bhatnagar, A.K. Minocha, M. Sillanpää, Adsorptive removal of cobalt from aqueous solution by utilizing lemon peel as biosorbent, Biochem. Eng. J., 48 (2010) 181–186.

[34] M.R. Lasheen, N.S. Ammar, H.S. Ibrahim, Adsorption/desorption of Cd(II), Cu(II) and Pb(II) using chemically modified orange peel: equilibrium and kinetic studies, Solid State Sci., 14 (2012) 201–210.

[35] H. Chen, T. Yan, F. Jiang, Adsorption of Cr(VI) from aqueous solution on mesoporous carbon nitride, J. Taiwan Inst. Chem. Eng., 45 (2014) 1842–1849.

[36] A.H. Jawad, Y.S. Ngoh, K.A. Radzun, Utilization of watermelon (*Citrullus lanatus*) rinds as a natural low-cost biosorbent for adsorption of methylene blue: kinetic, equilibrium and thermodynamic studies, J. Taibah Univ. Sci., 12 (2018) 371–381.

[37] K.Y. Foo, B.H. Hameed, Preparation, characterization and evaluation of adsorptive properties of orange peel based activated carbon via microwave induced K_2CO_3 activation, Bioresour. Technol., 104 (2012) 679–686.

[38] T. Aman, A.A. Kazi, M.U. Sabri, Q. Bano, Potato peels as solid waste for the removal of heavy metal copper(II) from waste water/industrial effluent, Colloids Surf., B, 63 (2008) 116–121.

[39] C. Liu, H.H. Ngo, W. Guo, K.-L. Tung, Optimal conditions for preparation of banana peels, sugarcane bagasse and watermelon rind in removing copper from water, Bioresour. Technol., 119 (2012) 349–354.

[40] D.C. Panadare, V.G. Lade, V.K. Rathod, Adsorptive removal of copper(II) from aqueous solution onto the waste sweet lime peels (SLP): equilibrium, kinetics and thermodynamics studies, Desal. Water Treat., 52 (2013) 7822–7837.

[41] T.J. Mohammed, R.I. Ibrahim, Remediation of Cu(II) from well water of Iraq by using cortex of fruits and agricultural waste, Arabian J. Sci. Eng., 41 (2016) 345–355.

[42] H.M.F. Freundlich, Over the adsorption in solution, J. Phys. Chem., 57 (1906) 1100–1107.

[43] B.H. Hameed, H. Hakimi, Utilization of durian (*Durio zibethinus* Murray) peel as low cost sorbent for the removal of acid dye from aqueous solutions, Biochem. Eng. J., 39 (2008) 338–343.

[44] M.B. Desta, Batch sorption experiments: Langmuir and Freundlich isotherm studies for the adsorption of textile metal ions onto Teff Straw (*Eragrostis tef*) agricultural waste, J. Thermodyn., 2013 (2013) 1–6, doi: 10.1155/2013/375830.

[45] B.E. Reed, M.R. Matsumoto, Modelling cadmium adsorption by activated carbon using the Langmuir and Freundlich isotherm expressions, Sep. Sci. Technol., 28 (1993) 2179–2195.

[46] M.M. Dubinin, The Equation of the characteristic curve of activated charcoal, Dokl. Akad. Nauk. SSSR, 55 (1947) 327–329.

[47] D.N. Misra, Adsorption on heterogeneous surfaces: a Dubinin–Radushkevich equation, Surf. Sci., 18 (1969) 367–372.

[48] B.P. Bering, M.M. Dubinin, V.V. Serpinsky, On thermodynamics of adsorption in micropores, J. Colloid Interface Sci., 38 (1972) 185–194.

[49] D.Z. Husein, R. Hassanien, M.F. Al-Hakkani, Green-synthesized copper nano-adsorbent for the removal of pharmaceutical pollutants from real wastewater samples, Heliyon, 5 (2019) e02339, doi: 10.1016/j.heliyon.2019.e02339.

[50] X. Zhao, G. Zhang, Q. Jia, C. Zhao, W. Zhou, W. Li, Adsorption of Cu(II), Pb(II), Co(II), Ni(II) and Cd(II) from aqueous solution by poly(aryl ether ketone) cotaining pendant carboxyl groups (PEK-L): equilibrium, kinetics, and thermodynamics, Chem. Eng. J., 171 (2011) 152–158.

[51] S. Mustafa, M. Irshad, M. Waseem, K.H. Shah, U. Rashid, W. Rehman, Adsorption of heavy metal ions in ternary ststems onto $Fe(OH)_3$, Korean J. Chem. Eng., 30 (2013) 2235–2240.

[52] O. Hamdaoui, Batch study of liquid-phase adsorption of methylene blue using cedar sawdust and crushed brick, J. Hazard. Mater., 135 (2006) 264–273.

[53] R.M. Kulkarni, K.V. Shetty, G. Srinikethan, Cadmium(II) and nickel(II) biosorption by Bacillus lateroporus (MTCC 1628), J. Taiwan Inst. Chem. Eng., 45 (2014) 1628–1635.

[54] W.S.W. Ngah, M.A.K.M. Hanafiah, Adsorption of copper on rubber (*Hevea brasiliensis*) leaf powder: kinetic, equilibrium and thermodynamic studies, Biochem. Eng. J., 39 (2008) 521–530.

[55] M. Campbell, Extraction of Pectin from Watermelon Rind, Oklahoma State University, 2006.